ARTICLE

Targeting SLP2-mediated lipid metabolism reprograming restricts proliferation and metastasis of hepatocellular carcinoma and promotes sensitivity to Lenvatinib

Yufeng Liu[1,6], Linmao Sun[1,6], Hongrui Guo[2,6], Shuo Zhou[2,6], Chunxu Wang[3,6], Changyong Ji[2,6], Fanzheng Meng[2], Shuhang Liang[4], Bo Zhang[4], Yubin Yuan[5], Kun Ma[1], Xianying Li[2], Xinyu Guo[1], Tianming Cui[2], Ning Zhang[1], Jiabei Wang [2✉], Yao Liu [2✉] and Lianxin Liu [1✉]

SLP2, a protein located on mitochondrial, has been shown to be associated with mitochondrial biosynthesis. Here we explored the potential mechanisms by which SLP2 regulates the development of hepatocellular carcinoma. SLP2 could bind to the c-terminal of JNK2 to affect the ubiquitinated proteasomal degradation pathway of JNK2 and maintain the protein stability of JNK2. The increase of JNK2 markedly increases SREBP1 activity, promoting SREBP1 translocation into the nucleus to promote de novo lipogenesis. Alteration of the JNK2 C-terminal disables SLP2 from mediating SLP2-enhanced de novo lipogenesis. YTHDF1 interacts with SLP2 mRNA in a METTL3/m^6A-dependent manner. In a spontaneous HCC animal model, SLP2/c-Myc/sgP53 increases the incidence rate of spontaneous HCC, tumor volume, and tumor number. Importantly, statistical analyses show that levels of SLP2 correlate with tumor sizes, tumor metastasis, overall survival, and disease-free survival of the patients. Targeting the SLP2/SREBP1 pathway effectively inhibits proliferation and metastasis of HCC tumors with high SLP2 expression in vivo combined with lenvatinib. These results illustrate a direct lipogenesis-promoting role of the pro-oncogenic SLP2, providing a mechanistic link between de novo lipogenesis and HCC.

INTRODUCTION

Hepatocellular carcinoma (HCC), one of the most common malignant tumors, is also the fourth leading cause of cancer-associated death worldwide [1]. HCC can cause over 600,000 deaths per year worldwide [2]. HCC is a complex tumor that is steadily rising in incidence. Moreover, since HCC has an insidious onset, only when the disease has progressed to an advanced stage can patients receive a confirmed diagnosis [3]. Although several treatments, such as immune therapy, have been developed to treat HCC, the overall survival (OS) and disease-free survival (DFS) for HCC are poor because of early recurrence and metastasis [4]. Therefore, it is essential to clarify the underlying biological mechanisms of HCC proliferation and metastasis and to uncover reliable therapeutic targets.

Metabolic reprogramming is an important hallmark of cancer cells [5]. Malignant cells often show a high demand for glucose and glutamine and exhibit anaerobic glycolysis and high lactate production. Moreover, lipid metabolism is altered in cancer cells. With elevated lipogenesis and lipid β-oxidation, lipid metabolic reprogramming has a very large impact on malignant cells [6]. Lipids in cancer cells contain triglycerides (TGs), free fatty acids (FFAs), phospholipids (PLs), glycerophospholipids (GPs), sphingolipids, and cholesterol. Lipids can supply energy via fatty acid oxidation, form the cell membrane, and participate in biological processes as biomolecules termed lipid mediators [7]. The liver is the main organ for the synthesis of fatty acids, cholesterol, and PLs in the human body [8]. Lipid metabolism plays an important role in liver biological processes [9]. Since HCC cells are developed from normal hepatocytes, they often show dysregulation of lipid metabolism because of oncogene mutations [10]. Abnormally enhanced lipid metabolism can facilitate the proliferative and metastatic capacity of tumor cells via multiple signaling pathways [11]. Thus, discovering the molecules involved in these signaling pathways is crucial and may identify potential therapeutic targets.

Stomatin-like protein 2, also known as SLP2, is located on the mitochondrial and regulates mitochondrial biogenesis and mitochondrial functions, which include reactive oxygen species (ROS) and ATP generation [12, 13]. Its structure is similar to that of

[1]Department of Hepatic Surgery, Key Laboratory of Hepatosplenic Surgery, Ministry of Education, The First Affiliated Hospital of Harbin Medical University, Harbin 150001, China. [2]Department of Hepatobiliary Surgery, The First Affiliated Hospital of USTC, Division of Life Sciences and Medicine, Anhui Province Key Laboratory of Hepatopancreatobiliary Surgery, Anhui Provincial Clinical Research Center for Hepatobiliary Diseases, University of Science and Technology of China, Hefei 230001, China. [3]Department of Hematology, The First Affiliated Hospital of Harbin Medical University, Harbin 150001, China. [4]Department of Gastrointestinal Surgery, Anhui Province Key Laboratory of Hepatopancreatobiliary Surgery, The First Affiliated Hospital of USTC, Division of Life Sciences and Medicine, University of Science and Technology of China, Hefei 230001, China. [5]Department of Hepatobiliary Surgery, Heze City Hospital, Heze 274000, China. [6]These authors contributed equally: Yufeng Liu, Linmao Sun, Hongrui Guo, Shuo Zhou, Chunxu Wang, Changyong Ji. ✉email: jbwang16@ustc.edu.cn; liuyao66@ustc.edu.cn; liulx@ems.hrbmu.edu.cn

stomatin, but SLP2 does not contain an NH_2-terminal hydrophobic domain [14, 15]. Currently, some studies have reported that SLP2 is involved in the proliferation, metastasis, and adhesion of several cancer cell types [16–18]. By analyzing an esophageal squamous cell carcinoma cDNA microarray, SLP2 was shown to be one of the most differentially expressed genes in tumor tissue compared to normal tissue [19]. SLP2 can bind PHB to activate the MAPK pathway and thus promote gastric cancer progression, which may accelerate tumor growth [20, 21]. SLP2 is also considered a mitophagy regulator since it can regulate mitophagy by interacting with and promoting the stability of the PINK1 protein, which can facilitate cancer metastasis and drug resistance [22]. Moreover, SLP2 has recently been shown to play a role in promoting lung cancer as well as glioma [16, 23]. Although several studies have revealed that SLP2 can promote tumor development, its underlying biological function and signaling pathway have not been thoroughly clarified. Whether and how SLP2 is involved in cancer metabolic reprogramming still needs to be unveiled.

In this study, by using a single-cell database and comparing HCC tissue with peri-tumor tissue, SLP2 was found to be highly expressed in HCC tissue. HCC patients with high SLP2 expression have worse survival and a poorer prognosis than those with low SLP2 expression. We demonstrated that SLP2 can facilitate HCC proliferation and metastasis by enhancing lipid metabolism. The pro-tumor capacity of SLP2 in HCC is probably attributed to the binding of SLP2 to JNK2 and its ability to reduce the ubiquitination of JNK2, maintaining the stability of JNK2, which further facilitates the translocation of mature SREBP-1 into the nucleus. Remarkably, combined therapy with Lenvatinib and Fatostatin received best efficiency in HCC with high SLP2 expression. Moreover, the expression of SLP2 is regulated by METTL3 and YTHDF1 in a manner dependent on m^6A modification. These findings could provide a viable treatment strategy for one specific type of HCC and improve the efficacy of clinical treatment.

RESULT
SLP2 is aberrantly expressed in HCC and results in a poor prognosis
To discover the genes correlated with the development of HCC, HCC single-cell sequencing data (GSE125449) from Tumor Immune Single-cell Hub (TISCH) was analyzed (Supplementary Fig. 1A). We screened for genes that are specifically highly expressed in tumors ($\log_2FC > 2$) than in other tissues. After locating these genes, we focused on 89 genes that may affect tumor progression through metabolic pathways. We also analyzed differentially expressed genes in HCC in the TCGA and GEO databases. Combining the above results, two differentially expressed genes were selected, SLP2 and HMGCS2. (Fig. 1A, B). We validated the expression profiles of the above two genes, and we found that SLP2 was highly expressed in most cancers and was correlated with poor OS and DFS, while the expression of HMGCS2 varied widely among cancers (Supplementary Fig. 1B–D). Therefore, we focused on the mitochondria-related protein SLP2 for further study. The protein expression levels of SLP2 were validated in patients with HCC ($n = 36$) (Supplementary Table 3), which is consistent with the results from the analysis of the GEPIA database (Fig. 1C). To further verify SLP2 expression in HCC patients, immunohistochemical staining was performed with SLP2 antibodies in microarrays of 100 HCC patients. In HCC tissues, the overall positive rate of SLP2 was 80% (80/100), which was much higher than the 24% (24/100) observed in peri-tumor tissues. Moreover, the expression of SLP2 was higher in advanced HCC than in lower-stage tumors (Fig. 1D). Then, according to the IHC score, cases were separated into the SLP2 high expression group and the SLP2 low expression group by the immunohistochemical staining score. Clinicopathological characterization showed that high expression of SLP2 was associated with TNM stage

($P = 0.0017$), vascular invasion ($P = 0.0028$), and tumor size ($P < 0.0001$) (Fig. 1E). These data suggest that upregulation of SLP2 is closely associated with HCC.

We next evaluated the correlation between SLP2 and HCC prognosis. According to the TCGA database, we analyzed the survival of patients with high SLP2 expression and those with low SLP2 expression, and Kaplan–Meier curve analysis showed that patients with higher SLP2 expression had a worse OS ($P = 0.018$) and DFS ($P = 0.045$) (Supplementary Fig. 1D). Interestingly, HCC patients in cohort 1 ($n = 100$) with a worse OS ($P = 0.0029$) and DFS ($P = 0.0191$) usually had higher SLP2 expression (Fig. 1F). These results demonstrate that SLP2 expression is elevated in HCC tissues and that SLP2 can be considered a molecule to predict patient prognosis.

SLP2 promoted HCC cell proliferation, migration, and invasion in vivo and in vitro
Considering that the abnormal expression of SLP2 is highly correlated with the malignancy of HCC, we validated the function of SLP2 in HCC cells through both in vivo and in vitro assays. Before functional assays, SLP2 protein expression levels and mRNA expression levels in HCC cell lines were confirmed. Compared to those in normal liver cells (L-02), higher protein expression levels and mRNA levels of SLP2 were detected in the Hep-3B and HCCLM3 cell lines. Meanwhile, SMMC-7721 and Huh-7 cells showed lower SLP2 expression (Fig. 2A, B). Next, we designed gain-of-function and loss-of-function assays by lentiviral transfection to overexpress SLP2 in SMMC-7721 and Huh-7-cell lines and downregulate SLP2 expression in HCCLM3 and Hep-3B cell lines. For the knockdown experiments, three shRNAs (SLP2-sh#1, SLP2-sh#2, SLP2-sh#3) were used to infect HCCLM3 and Hep-3B cells. After transfection, the efficiency of the shRNAs were verified through western blotting and qRT–PCR (Supplementary Fig. 2A, B). Because SLP2-sh#1 and SLP2-sh#3 showed a higher knockdown efficiency, these two shRNAs were chosen as the best candidates for silencing SLP2. The efficiency of lentivirus-mediated overexpression was likewise validated (Supplementary Fig. 2B). These stable cell lines were used for the following experiment.

We next verified whether SLP2 has a role in promoting the proliferation of HCC. Clone formation analysis showed that SLP2 overexpression increased colony number, whereas knocking down SLP2 impaired colony formation (Fig. 2C and Supplementary Fig. 2C). The 3D spheroid-formation culture test also showed that SLP2 overexpression increased the proliferative capacity of HCC (Fig. 2D). We also verified these findings in vivo. For subcutaneous implantation animal models, subcutaneous tumor size was measured every 4 days. When tumors were harvested, they were compared with those from the control group. Huh-7-SLP2 cells were more likely to have faster growth rates and larger tumor volumes, while HCCLM3-sh-SLP2 cells showed reduced tumorigenicity (Fig. 2E). In addition, overexpression of SLP2 led to enhanced Ki67 staining in tumor sections, while silencing SLP2 expression weakened Ki67 staining (Supplementary Fig. 2D).

To clarify whether SLP2 is involved in the metastasis of HCC cells, Transwell assays and wound healing assays were performed. Transwell migration and Matrigel invasion assays showed that knockdown of SLP2 in HCCLM3 and Hep-3B cell lines reduced their motility and invasive behaviors, whereas overexpression of SLP2 significantly promoted the above abilities (Supplementary Fig. 3A, B). Similar results were observed in wound healing assays (Fig. 2F, G). Cell migratory capacity was enhanced when SLP2 was upregulated in Huh-7 and SMMC-7721 cells. In contrast, this ability was abolished when SLP2 was silenced (Supplementary Fig. 3C).

To verify whether SLP2 can affect the metastasis of HCC in vivo, we injected stable cell lines (HCCLM3-shSLP2, HCCLM3-ctrl, Huh-7-SLP2, and Huh-7 vector) into the tail veins of nude mice. After 6 weeks, the lungs were harvested. Mice in the Huh-7-SLP2 group demonstrated more and larger metastatic nodules than the mice
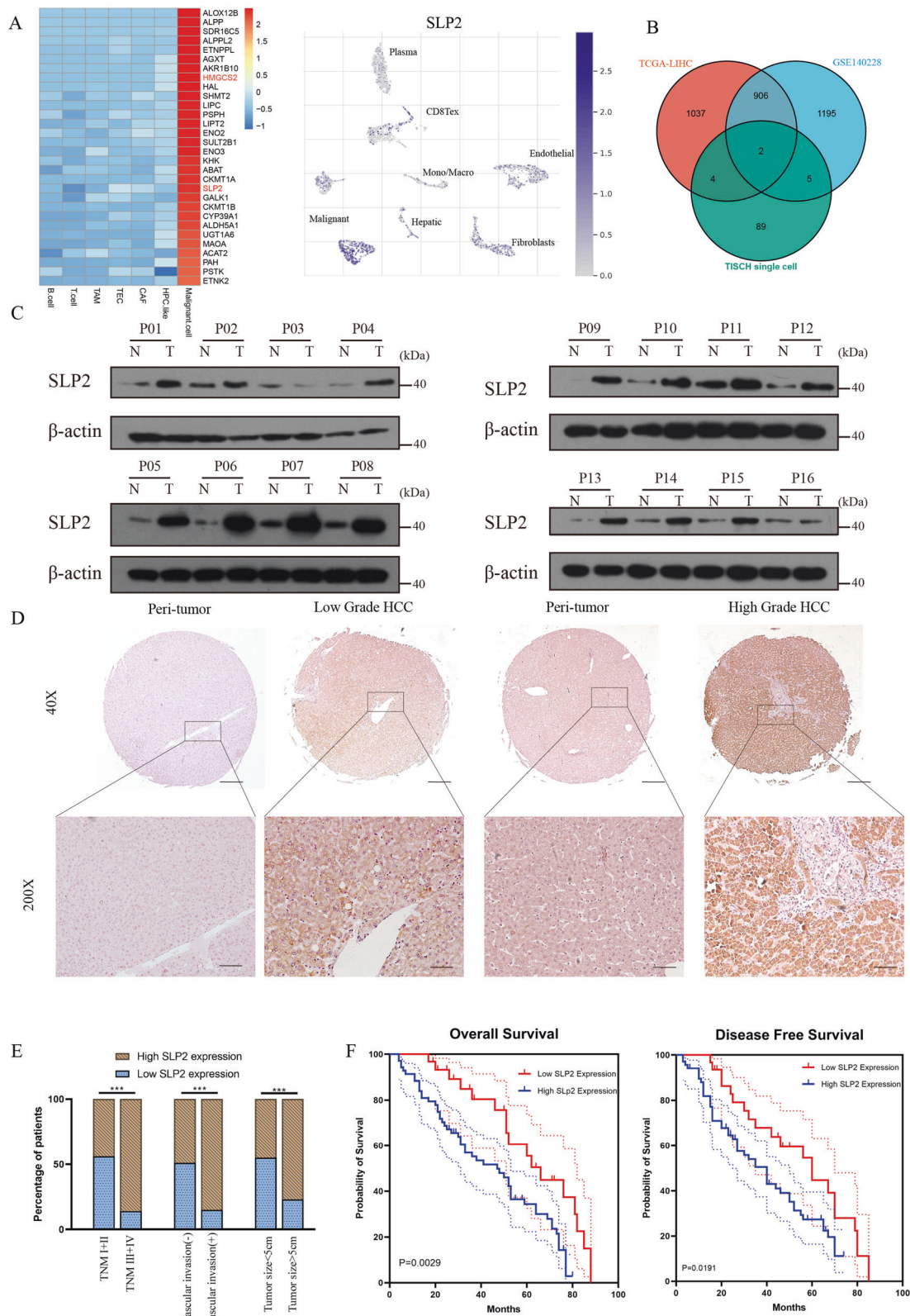
Fig. 1   SLP2 is frequently upregulated in HCC and is a promising prognostic biomarker for HCC. A Gene heatmap in TISCH and SLP2 expression abundance in each subgroup. **B** The most significantly differentially expressed genes were screened from the TCGA database, GEO database, and TISCH single-cell database. **C** Representative images following Western blotting of SLP2 in HCC tissues and adjacent peri-tumor tissues. P patient, T tumors, N: peri-tumor normal tissues. **D** Representative images of SLP2 IHC staining in HCC tissues and normal liver tissues. Scale bars 50 μm, up panel. 25 μm, down panel. **E** Percentage of patients with relatively high expression and low expression of SLP2 according to the following clinical parameters:, (1) tumor TNM stage (2) vascular invasion and (3) tumor size. **F** Kaplan–Meier plot of OS and DFS of patients with HCC with relatively high or low SLP2. All experiments were performed three times, and the data are presented as the mean ± SD. *$p < 0.05$; **$p < 0.01$; ***$p < 0.001$.
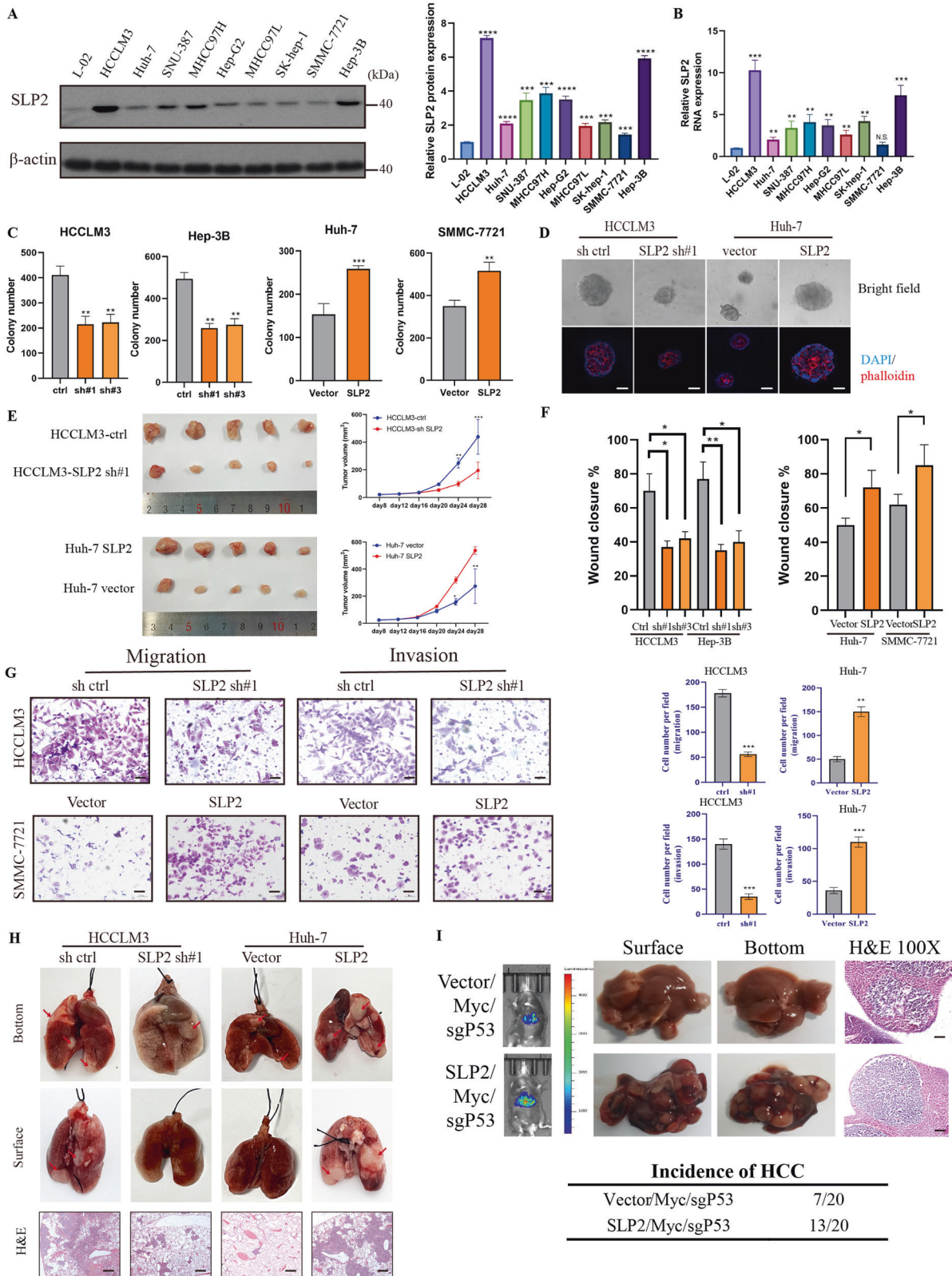
in the Huh-7 vector group, whereas, in the HCCLM3 cell line, knockdown of SLP2 led to a reduction in lung metastatic nodules (Supplementary Fig. 3D). The metastatic nodules were verified by H&E staining (Fig. 2H). These results provide further evidence that SLP2 could promote invasion and metastasis in HCC.

To further clarify the enhanced tumorigenicity of SLP2-overexpressing HCC cells, we constructed a pT3-EF1a plasmid for the co-expression of SLP2 or myc and pX330 vectors for the coexpression of sgRNAs targeting P53. In addition, to specifically target the plasmid to the liver, the CMV-Sleeping beauty-13

Fig. 2 SLP2 enhances HCC cell proliferation, migration, and invasion in vivo and in vitro. A Western blot analysis of SLP2 expression in normal liver cells and HCC cells. **B** Relative SLP2 protein and mRNA expression in HCC cells compared to normal liver cells. **C** Statistical analysis of colony formation assay data. **D** Representative images of the 3D spheroid-formation assay data for the indicated cells (200×), Red: phalloidin, blue: DAPI. **E** Representative images of subcutaneous xenografts derived from the indicated HCC cells and the change in tumor volume in the subcutaneous model. **F** Statistical analysis of wound healing assays. **G** Representative images of Transwell migration and Matrigel invasion assays for the indicated cells (100×). Statistical analysis of the Transwell assay data from three independent experiments, scale bar: 50 μm. **H** Representative images of lung metastasis specimens; The nodules were marked with red arrows, H&E-stained images of lung metastasis in the indicated groups. **I** Images of bioluminescence pictures and H&E staining of vector/c-Myc/sgP53 and SLP2/c-Myc/sgP53 C57BL mouse livers at 8 weeks after hydrodynamic injection. Scale bars, 50μm All experiments were performed three times, and the data are presented as the mean ± SD. *$p < 0.05$; **$p < 0.01$; ***$p < 0.001$. ****$p < 0.0001$.
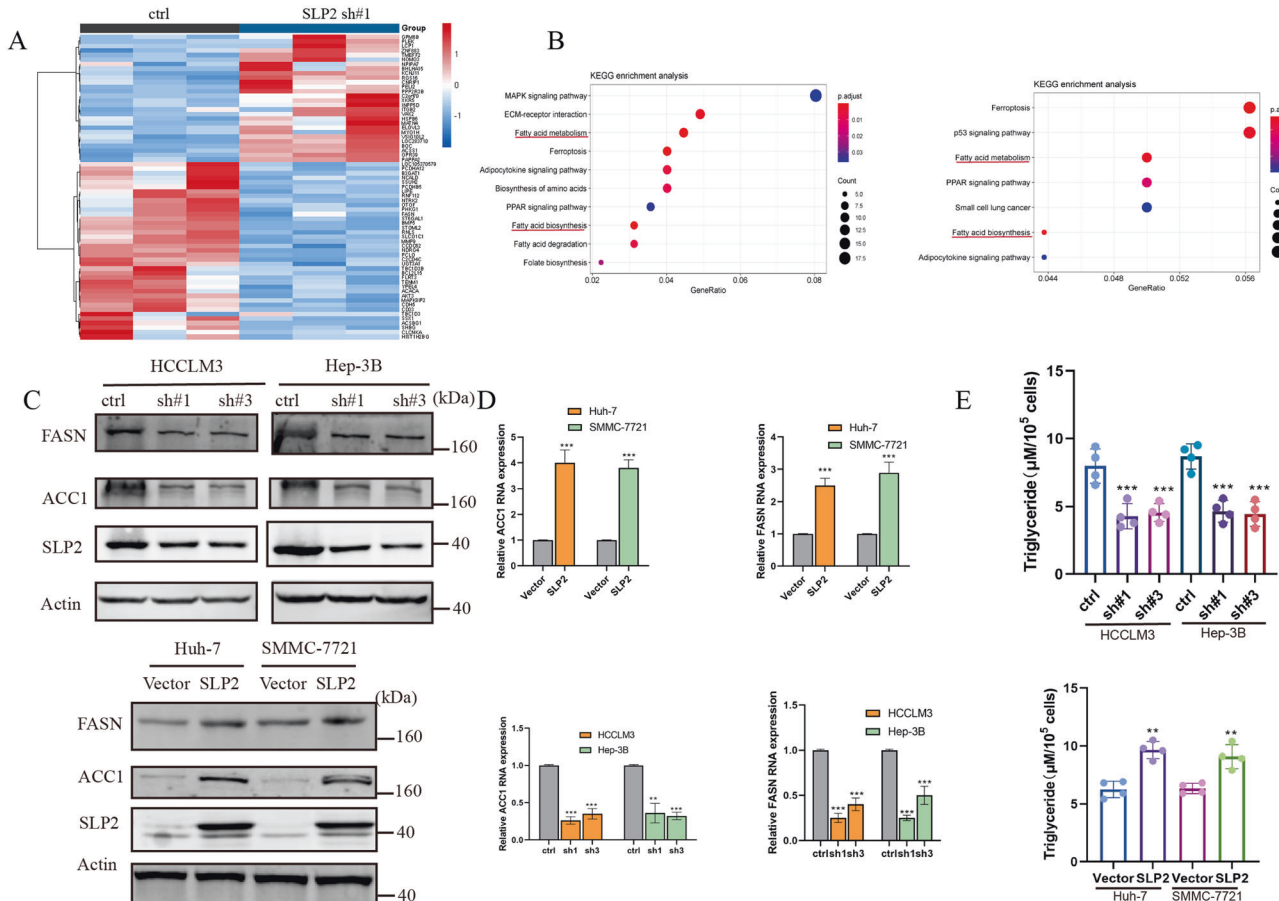

Fig. 3 SLP2 could affect tumor progression through lipid metabolism. A Heatmap of RNA sequencing data for ctrl and shSLP2 HCC cell lines. **B** KEGG enrichment analysis of SLP2-regulated genes. The two sets of results are marked with red lines where they overlap. Sh-SLP2 group(left) SLP2 overexpression group(right). **C** Western blot analysis for FASN, ACC1, and SLP2 in the indicated cells. **D** Relative FASN and ACC1 mRNA expression in HCC cells transfected with lentivirus compared to the control group. **E** Quantitative measurement of TGs in the indicated cell lines.

plasmid was used. By hydrodynamic tail vein injection with vector/c-Myc/sgP53 and SLP2/c-Myc/sgP53, we established an SLP2 overexpression HCC animal model (20 mice/group). The results showed that SLP2 overexpression increased the incidence of HCC, tumor volume, and tumor number caused by c-Myc overexpression and P53 knockout (Fig. 2I). In summary, our findings suggest that SLP2 is crucial in promoting HCC growth in vitro and tumor formation in vivo.

SLP2 may affect tumor progression through lipid metabolism
Since overexpression and knockdown of SLP2 significantly affected the biological properties of HCC cell lines, RNA sequencing of these stable cell lines was performed to identify the differentially expressed genes after SLP2 overexpression or knockdown (Fig. 3A and Supplementary Fig. 4A). KEGG pathway enrichment analysis was performed afterward (Fig. 3B). Fatty acid

metabolism and fatty acid biosynthesis pathways emerged in both the knockdown group and the overexpression group. We, therefore, searched for the specific lipid metabolism-related genes whose expression was associated with SLP2. Among the key enzymes that have an impact on lipid metabolism, Fatty Acid Synthase (FASN) ($P < 0.0001$) and Acetyl Coenzyme A Carboxylase 1 (ACC1) ($P = 0.005$), which are related to lipid synthesis, were elevated significantly, while there were no significant changes in carnitine palmitoyltransferase, a key enzyme for fatty acid oxidation (Supplementary Fig. 4A).

Therefore, to verify these findings, we examined the expression levels of the key enzymes involved in de novo lipogenesis. The results showed that in SLP2 knockdown cell lines, the expression of FASN and ACC1 was reduced, while in SLP2-overexpressing cell lines, the protein levels of FASN and ACC1 were elevated (Fig. 3C). The above results were further validated by qRT–PCR (Fig. 3D).
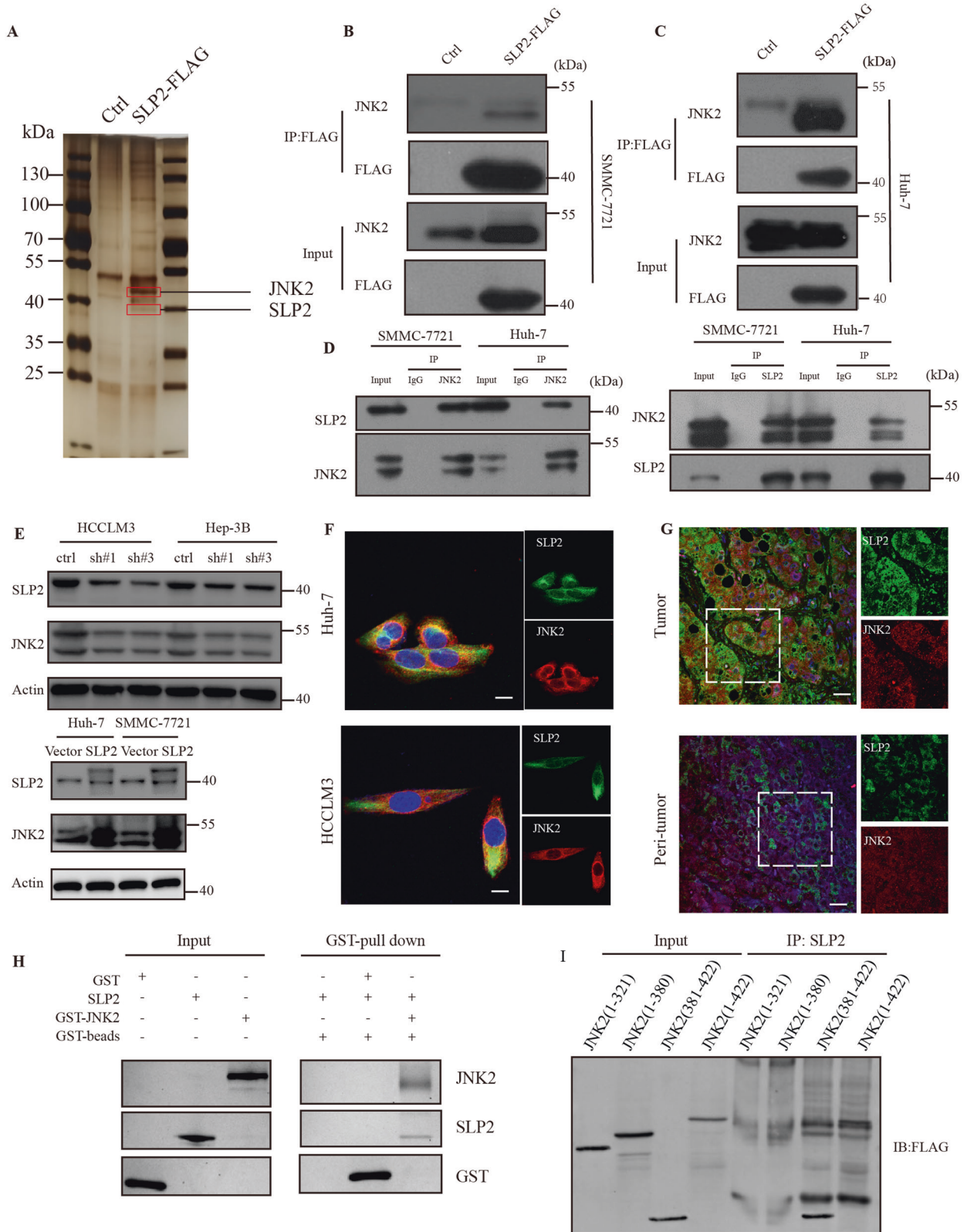
This result was also validated in data from 367 patients in the TCGA database (Supplementary Fig. 4B). The expression of FASN and ACC1 was also clarified in 40 tissue samples, and correlation analysis showed a positive correlation between the expression of FASN/ACC1 and SLP2 (Supplementary Fig. 4C). The expression of

FASN and ACC1 in the TCGA database showed the same trend (Supplementary Fig. 4D). TGs are crucial components in the de novo lipid synthesis of fatty acids, and TG levels were detected in SLP2 knockdown and overexpression HCC cell lines. The results suggested that the TG content decreased when SLP2 expression

Fig. 4 SLP2 could interact with the C-terminus of JNK2. A Total-cell lysate was extracted from SLP2-FLAG-overexpressing HCC cells or control cells, pulled down by anti-FLAG beads and resolved by SDS–PAGE. The silver-stained gel showed differential bands, and the identified JNK2 peptide is shown. **B**, **C** SMMC-7721 and Huh-7 cells were transfected with SLP2-FLAG or empty vector and subjected to immunoprecipitation using anti-FLAG mAb. Coimmunoprecipitated JNK2 was detected using an anti-JNK2 antibody. **D** Endogenous SLP2 in HCCLM-3 and Hep-3B cells was immunoprecipitated using an anti-SLP2 antibody with rabbit IgG as a nonspecific control. Coimmunoprecipitated JNK2 was detected using an anti-JNK2 antibody. **E** Western blot analysis of JNK2 in the indicated cells. **F**, **G** The expression and colocalization of SLP2 and JNK2 were analyzed in HCC cell lines as well as HCC tissues and peri-tumor liver tissue of HCC patients by confocal microscopy. (Scale bar: 25 μm). **H** Purified SLP2 and GST-JNK2 were co-incubated, and bound proteins were pulled down by anti-GST beads. **I** IP assays for SLP2 and JNK2 proteins with different lengths.

was reduced, whereas the TG content increased when SLP2 expression was increased (Fig. 3E). This result clarifies that SLP2 may be related to the de novo synthesis of fatty acids in HCC cells.

SLP2 could interact with JNK2 and maintain the protein stability of JNK2

To reveal the molecular mechanism by which SLP2 regulates lipid metabolism in HCC cells, immunoprecipitation/mass spectrometry (IP/MS) was used to discover proteins or peptides that may interact with SLP2. In both the Huh-7 and SMMC-7721 cell lines, SLP2-FLAG was overexpressed and immunoprecipitated with an anti-FLAG mAb. Silver staining was used to identify proteins that might bind SLP2 (Fig. 4A), and the specific bands were analyzed by mass spectrometry. To account for the heterogeneity of tumor cells, proteins that appeared in both sets of results were selected as candidate proteins. We identified JNK2 in mass spectrometry analysis, which may be related to lipid metabolism. A coimmunoprecipitation assay was carried out to confirm whether SLP2 can interact with JNK2. JNK2 was detected in anti-FLAG bead precipitates but could not be detected in the control group (Fig. 4B, C). Furthermore, endogenous immunoprecipitation was likewise performed to confirm that JNK2 could indeed bind SLP2 (Fig. 4D). Because of the structural similarity of JNK1 and JNK2, we also tested whether JNK1 could bind SLP2, but the results showed that JNK1 does not interact with SLP2 (Supplementary Fig. 5A, B).

We next investigated whether SLP2 affects the protein expression of JNK2. The results showed that knockdown or overexpression of SLP2 resulted in the same change in the protein levels of JNK2 but no significant changes at the mRNA level (Fig. 4E and Supplementary Fig. 5D). Demonstrating that JNK2 is located downstream of SLP2, the protein level of SLP2 was not changed after JNK2 was knocked down (Supplementary Fig. 5C). To bolster this conclusion, we observed the intracellular localization of SLP2 and JNK2 in HCC cells using laser confocal microscopy, and we found colocalization of SLP2 and JNK2 in HCC cell lines (Fig. 4F and Supplementary Fig. 5E, F). Similar colocalization was found in HCC tissues with high SLP2 expression. However, this colocalization effect was not apparent in peri-tumor tissues (Fig. 4G). Therefore, to further prove that JNK2 can indeed bind SLP2, GST pull-down experiments were performed to verify this conclusion. Interestingly, the data showed that JNK2 could bind SLP2 (Fig. 4H).

To further explore the SLP2-binding site in JNK2, we analyzed the protein sequence of JNK2, which contains a total of 422 amino acids. We found that the tertiary structure of JNK2 consists mainly of a tyrosine-containing catalytic structural domain (1-380) that can undergo phosphorylation, which is relatively conserved and can activate MAP kinases. JNK1 and JNK3 also have the same catalytic structural domain. Amino acids containing a ubiquitination site are located in the JNK2 C-terminus. The amino acid sequence of the JNK1 protein differs markedly from that of JNK2 at the C-terminus. We, therefore, designed plasmids containing JNK2 sequences of different lengths and transferred them into HEK293T cells to determine which peptides could still bind SLP2 after validation by IP experiments. We found that deletion of the 42 amino acids in the C-terminus of JNK2, but not the N-terminus,

abolished its interaction with SLP2. Combined with the previous results, we found that JNK2 binds SLP2 through the 42 amino acids in the C-terminus (Fig. 4I).

After analyzing the above findings, we hypothesized that SLP2 regulates JNK2 at the protein level. We next explored whether SLP2 can affect the protein stability of JNK2. The results showed that the rate of JNK2 degradation in SLP2 knockdown cell lines increased after the addition of the protein synthesis inhibitor cycloheximide (Fig. 5A). Moreover, the proteasome-specific inhibitor MG132 protected against JNK2 protein degradation in HCC cells with low SLP2 expression (Fig. 5B), while after the use of the autophagy inhibitor Baf-A1, there were no significant changes in the protein levels of JNK2 (Supplementary Fig. 5G, 6A). We, therefore, investigated the level of ubiquitination of JNK2 protein in HCC cells with different SLP2 expression levels. JNK2 protein in SLP2-overexpressing cells tended to show a significant reduction in polyubiquitination, while the opposite was observed upon transfection with SLP2 sh#1 and SLP2 sh#3 in HCCLM3 cells. The data above demonstrated that SLP2 could suppress the degradation of JNK2 (Fig. 5C). The above results clarify that SLP2 inhibits the ubiquitination of JNK2 by binding JNK2, promoting the stability of the JNK2 protein.

SLP2 could regulate SREBP1-mediated lipid metabolism through JNK2

Considering that SLP2 may affect tumor progression through lipid metabolism, wide-target lipid metabolomics was performed. A total of 956 metabolites, including TGs, FFAs, PLs, glycerophospholipids (GPs), sphingolipids, and cholesterol, were detected. The data demonstrated that TGs and fatty acid metabolites were significantly reduced after SLP2 was knocked down. When SLP2 was overexpressed, multiple types of lipid synthesis became more active. These results suggest that SLP2 can indeed promote lipid metabolism, especially lipid synthesis, in HCC cells (Fig. 5D). The accumulation of intracellular lipids may be due to increased external uptake or otherwise increased internal synthesis. Since normal liver cells are naturally characterized by de novo lipogenesis, we hypothesized that HCC cells with high SLP2 expression increase lipid content via de novo lipogenesis.

We stained SLP2-overexpressing and SLP2 knockdown cell lines with the lipophilic dye BODIPY 493/503 to observe the correlation between SLP2 and the intracellular lipid content. The data showed that when SLP2 expression was downregulated, the number of intracellular lipid droplets decreased, and conversely, when SLP2 expression was elevated, the number of intracellular lipid droplets increased. Notably, this effect was attenuated when JNK2 was knocked down in SLP2-overexpressing HCC cells (Fig. 5F, G, Supplementary Fig. 6B). This conclusion was also supported by the results of flow cytometry (Fig. 5E). Moreover, this phenomenon was eliminated by adding JNK2 inhibitors to SLP2-overexpressing cell lines (Supplementary Fig. 7A). Taken together, SLP2 can promote the reprogramming of lipid metabolism in HCC via JNK2.

As a result of mass spectrometry analysis, SREBP1 could also be pulled down by anti-FLAG beads (Supplementary Fig. 7B). Since SREBP1 plays a crucial role in lipid metabolism, we also verified the ability of SREBP1 to bind SLP2 using co-IP. The results showed that
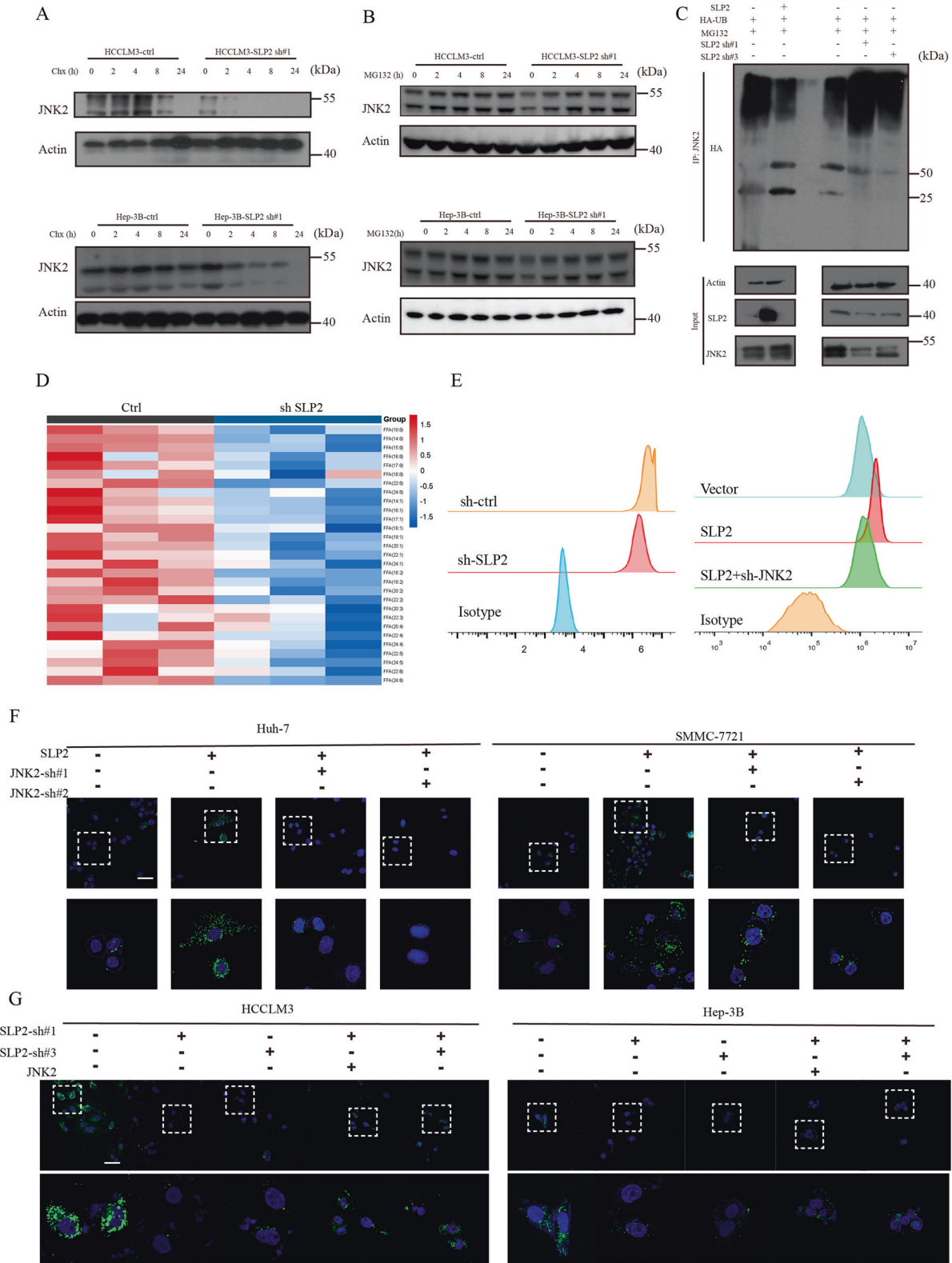
SREBP1 could be detected in the precipitates, but SREBP2 could not (Fig. 6A and Supplementary Fig. 7C, E). As it has been reported that JNK2 can bind SREBP1 [24], we supposed that SREBP1 and SLP2 are indirectly bound through JNK2. After knocking down JNK2, SREBP1 could not be pulled down by anti-FLAG beads

(Fig. 6B). The numerous lines of the evidence above proved the correlation between SLP2/JNK2 and SREBP1, which was confirmed by the assays performed above. We next examined whether the expression levels of SREBP1 were associated with SLP2 at the mRNA and protein levels. The qRT–PCR results showed no

Fig. 5 SLP2 could maintain the protein stability of JNK2 and regulate SREBP1-mediated lipid metabolism through JNK2. **A** Downregulation of SLP2 led to accelerated degradation of JNK2. Western blot analysis detected alterations in JNK2 in Hep-3B and HCCLM3 cells treated with 25 μM MG132. **B** Western blot analysis detected alterations in JNK2 in Hep-3B and HCCLM3 cells treated with 10 μg/ml CHX for the indicated times. **C** Overexpression of SLP2 in Huh-7 cells increased the accumulation of polyubiquitinated JNK2 after treatment with MG132. Knockdown of SLP2 in HCCLM3 cells reduced polyubiquitinated JNK2. JNK2 was pulled down, and an anti-HA antibody was used to detect polyubiquitinated JNK2. **D** Heatmap showing GC–MS-based lipid analysis of HCC cells bearing sh-SLP2. **E** Quantitative measurement of intracellular neutral lipids using flow cytometry to detect the fluorescence intensity of BODIPY 493/503. **F, G** The content of neutral lipids was detected by double staining with BODIPY 493/503 dye and DAPI in the indicated cells. Scale bars, 25 μm. All experiments were performed three times, and the data are presented as the mean ± SD. *$p < 0.05$; **$p < 0.01$; ***$p < 0.001$. ****$p < 0.0001$.

significant differences in SREBP1 at the transcriptional level (Supplementary Fig. 7F). At the protein expression level, we found increased accumulation of mature SREBP1 in cell lines over-expressing SLP2 by Western blotting using a specific anti-SREBP1 antibody. In addition, when a JNK2 inhibitor was applied to SLP2-overexpressing cells, mature SREBP1 levels decreased again (Fig. 6C). The same phenomenon was observed when JNK2 was knocked down in SLP2-overexpressing cell lines. We next verified whether the key enzymes for de novo lipogenesis would show the same changing trend. The data showed that inhibiting JNK2 with JNK2 inhibitors or silencing JNK2 eliminated the lipid metabolism-promoting effect of SLP2 (Fig. 6D).

After verifying the increased expression levels of enzymes related to fatty acid metabolism, we measured the intracellular levels of metabolites containing PLs, TGs, lactic acid, and ATP in HCC cells. When the expression level of SLP2 was reduced, the intracellular PL and TG contents were subsequently reduced. When SLP2 was overexpressed, the intracellular PL and TG contents increased. Notably, JNK2 inhibitors downregulated the TG and PL contents in SLP2-overexpressing cell lines (Fig. 6E). In addition, there was no significant correlation between the lactate content and the expression level of SLP2 or the application of JNK inhibitors (Supplementary Fig. 7D). The intracellular ATP content was positively correlated with SLP2 expression levels, while this trend could be eliminated by JNK2 inhibitors (Fig. 6E). We have found elevated expression of ACC1 and FASN in HCC cell lines overexpressing SLP2. After the application of inhibitors of SREBP1, the expression of FASN and ACC1 was downregulated. These data demonstrated that nuclear translocation of SREBP1 regulates their transcription. (Supplementary Fig. 7G).

SLP2 and JNK2 together promote the translocation of mature SREBP1 to the nucleus
To examine SREBP1 activation in HCC cell lines and HCC specimens, the localization of SLP2 and SREBP1 was observed using confocal microscopy. The results showed that SREBP1 was distributed in the cytoplasm and nucleus. However, significant nuclear translocation of SREBP1 was observed in SLP2-overexpressing cells, and most SREBP1 was localized in the nucleus. Moreover, this phenomenon was eliminated by adding JNK2 inhibitors to SLP2-overexpressing cell lines (Fig. 6G). Concerning the patient HCC specimens, TSA IF staining was performed to verify the colocalization of SLP2, JNK2, and SREBP1. The results indicated that more SREBP1 was localized in the nucleus in HCC tumor tissues than in adjacent tissues, along with increased expression and colocalization of JNK2 and SLP2 (Fig. 6F, Supplementary Fig. 8A). Colocalization of JNK2 and SREBP1 was also observed in HCC cell lines (Supplementary Fig. 8B). These data indicated that the nuclear translocation of SREBP1 was increased in both HCC cell lines and HCC tissues, which may be related to regulation via SLP2 and JNK2. Precursors of srebp1 are distributed in the cytoplasm, after cleavage by the Golgi, Mature SREBPs then translocate to the nucleus and bind as homodimers to the sterol regulatory elements (SREs) within the promoters of their target genes. Therefore, Precursor SREBP1 could interact with SLP2/JNK2 in cytoplasm. And up-regulated SLP2/JNK2 promotes cytoplasmic SREBP1 translocate into the nucleus.

To confirm the lipid metabolism regulated by SLP2 has the greatest impact on the regulation of tumor progression. SREBP1 was knocked down in SMMC7721-SLP2 and Huh-7-SLP2 cell lines (Supplementary Fig. 9A). After knockdown of SREBP1, the proliferation ability and metastatic ability of the above two types of hepatocellular carcinoma cells were attenuated. (Supplementary Fig. 9B–F).

The expression of SLP2 is regulated by METTL3 and YTHDF1
We found that SLP2 could interact with JNK2 as an oncogene to regulate lipid metabolism in HCC, but it is still unknown whether SLP2 is regulated by other upstream molecules. Through the m6A2target database, we found that the 3′UTR and the coding sequence (CDS) portions of the mRNA of SLP2 have multiple m^6A methylation sites. Based on the predicted results, we chose three m^6A writers, METTL3, METTL4, and VIRMA, that were most likely to modify SLP2 mRNA for validation. The expression of each of these three proteins was inhibited in an HCC cell line with corresponding small interfering RNAs. SLP2 expression decreased significantly when the expression of METTL3 was inhibited, while SLP2 decreased insignificantly when the other m^6A writers were knocked down (Fig. 7A). After reviewing the TCGA database, we found that METTL3 was positively correlated with SLP2 expression in 347 HCC patients. Moreover, compared to that in the peri-tumor tissues, METTL3 protein expression was higher in 347 HCC tissues (Fig. 7B).

It is known that m^6A readers can identify m^6A modification to regulate modified RNA biological functions. Recently, research has proven that some mRNA m^6A modifications can be recognized by YTHDF1. YTHDF1 can thus promote the translation of these target mRNAs. SLP2 was identified as a target mRNA of YTHDF1 through eCLIP-seq analyses (database GSE78030). Therefore, we examined whether YTHDF1 could recognize m6A-modified SLP2 mRNA and regulate its translation. To further test this hypothesis, RIP-qPCR was performed with an anti-YTHDF1 antibody to detect the interaction between the YTHDF1 protein and SLP2 mRNA in HCC cell lines. Obviously, there was significantly higher SLP2 enrichment in the anti-YTHDF1 group than in the anti-IgG control group (Fig. 7C). Moreover, when METTL3 was downregulated by siRNA, the interaction between YTHDF1 and SLP2 was disrupted, indicating that YTHDF1 interacts with SLP2 mRNA in a METTL3/m^6A-dependent manner (Fig. 7D). We, therefore, verified whether YTHDF1 could regulate the expression of SLP2. After knocking down YTHDF1, the expression level of SLP2 was downregulated (Fig. 7E). The mRNA level of SLP2 did not show a significant decrease, which means YTHDF1 could not stabilize SLP2 mRNA (Fig. 7F). In the TCGA HCC database, YTHDF1 was highly expressed in cancer and correlated with SLP2 expression (Fig. 7G). Collectively, these data suggest that METTL3 and YTHDF1 can regulate SLP2 expression.

Targeting the SLP2/SREBP1 pathway effectively inhibits proliferation and metastasis of HCC tumors with high SLP2 expression in vivo
Fatostatin is a newly found SREBP inhibitor that can directly bind SCAP (SREBP cleavage activating protein) and blocks SREBP
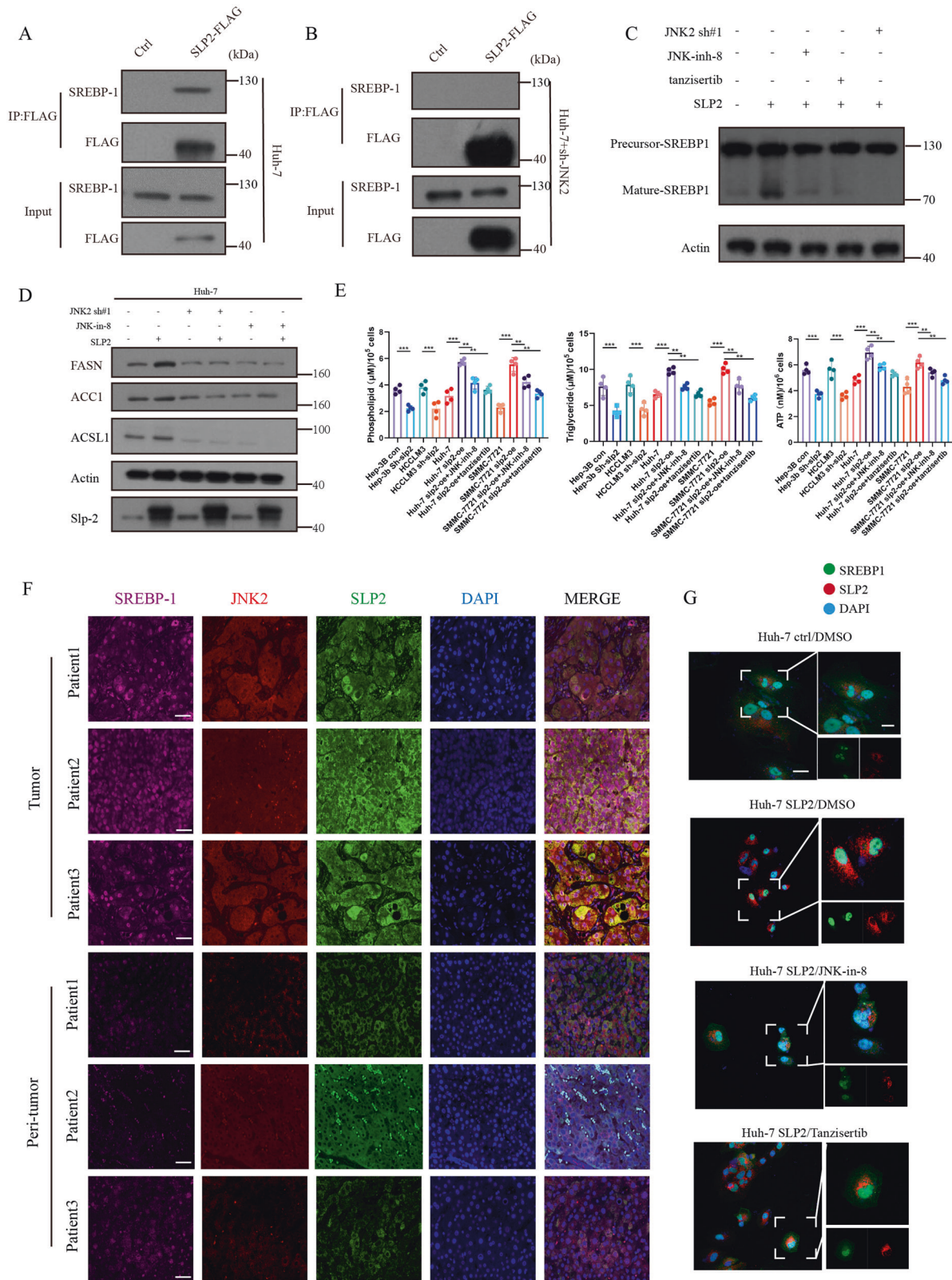
Fig. 6 SLP2 and JNK2 together promote the translocation of mature SREBP1 to the nucleus. A, B Huh-7 cells were transfected with SLP2-FLAG or empty vector and subjected to immunoprecipitation using anti-FLAG mAb. Coimmunoprecipitated SREBP1 was detected using an anti-SREBP1 antibody. After JNK2 was silenced, coimmunoprecipitated SREBP1 could not be detected. **C** Western blot analysis of premature and mature SREBP1 in the indicated cells. **D** Western blot analysis for FASN, ACC1, and ACSL1 in the indicated cells. **E** The intracellular levels of metabolites containing PLs, TGs, and ATP in the indicated cells were measured with reagent kits. **F** Distribution of SLP2, JNK2, and SREBP1 in HCC tissues and normal liver tissues observed by TSA IF (scale bar: 25 μm). **G** The expression and colocalization of SLP2 and SREBP1 were analyzed in HCC cell lines (scale bar: 25 μm). All experiments were performed three times, and the data are presented as the mean ± SD. *$p < 0.05$; **$p < 0.01$; ***$p < 0.001$. ****$p < 0.0001$.
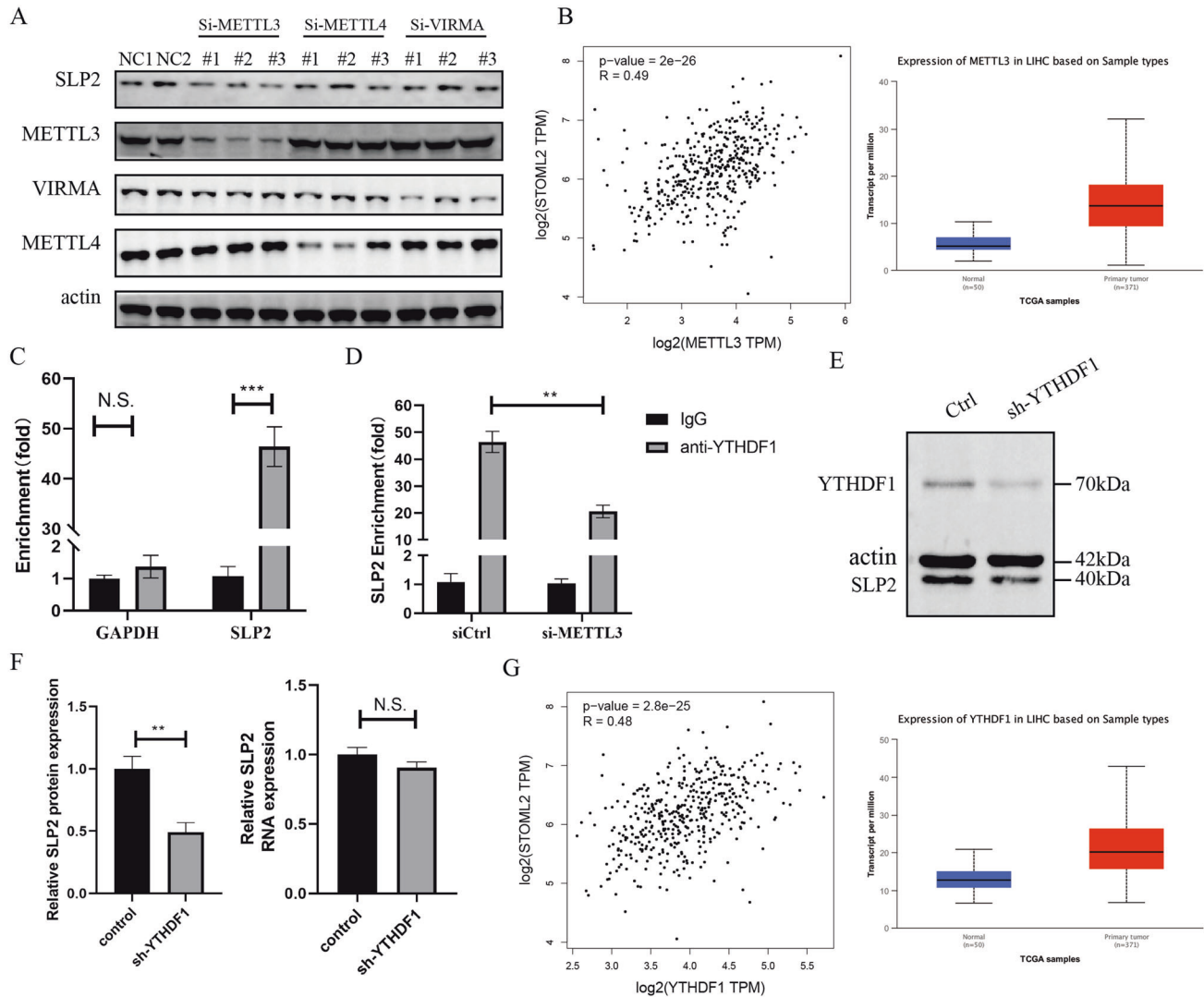
Fig. 7 Expression of SLP2 is regulated by METTL3 and YTHDF1. A Western blot analysis of SLP2 expression in the indicated cells transfected with siRNA. **B** Correlation of METTL3 and SLP2 expression levels in HCC tissues and METTL3 expression levels in HCC tissues and peri-tumor tissues. **C** RIP-qPCR analysis showing enrichment of YTHDF1 on SLP2 mRNA in HCC cells. IgG was used as an isotype control. GAPDH was used as a negative control. **D** RIP-qPCR analysis showing enrichment of YTHDF1 on SLP2 mRNA in control and si-METTL3 cells. IgG was used as an isotype control. **E** Western blot analysis of SLP2 and YTHDF1 expression in the indicated cells transfected with sh-YTHDF1. **F** Protein and mRNA expression levels of SLP2. **G** Correlation of YTHDF1 and SLP2 expression levels in HCC tissues and YTHDF1 expression levels in HCC tissues and peri-tumor tissues.

translocation to nuclear. Fatostatin is primarily indicated to block the activation process of SREBPs and thereby inhibit lipogenesis. The currently FDA-approved targeted drugs for first-line treatment of HCC are sorafenib and Lenvatinib. we first tested the effect of the above two drugs in combination with fatostatin in vitro. The results showed that fatostatin increased the sensitivity of hepatocellular carcinoma cells to the above two drugs. (Supplementary Fig. 10) Therefore, Fatostatin and Lenvatinib, currently the most used first-line chemotherapy drug in HCC, were used to evaluate the effect of inhibiting de novo lipogenesis on the proliferation and metastasis of HCC. To examine HCC growth, a subcutaneous tumor animal model was used. To examine HCC metastasis, a tail vein injection lung metastasis model was established. Cell line transfection, timeline, and treatments are described in Fig. 8A.

When comparing the tumor weights in each group (Fig. 8B), the tumor weight showed a significant decrease in Lenvatinib group (0.796 ± 0.108 g) and Lenvatinib+Fatostatin group(0.446 ± 0.102 g) compared to the blank group (1.34 ± 0.138 g). In addition, tumor weight and volume decreased more ($P < 0.001$) in Lenvatinib +Fatostatin group than in the lenvatinib alone group (Fig. 8C, D). And the difference between the blank group and the Fatostatin alone group was not significant. A lung metastasis model was used to assess the metastatic capacity of HCC. The Lenvatinib and Lenvatinib+Fatostatin significantly inhibited the metastatic ability of HCC cells (Fig. 8E). Both groups of mice treated with the Lenvatinib had significantly fewer metastatic nodules in the lungs than the blank group and Fatostatin group (Fig. 8F). Moreover, the nodules in Lenvatinib+Fatostatin is the fewest. After resection of subcutaneous tumors and metastatic nodules in each group of mice, TG levels were measured. Not surprisingly, tumors in blank and Lenvatinib group had higher TG content, and the application of the Fatostatin resulted in a decrease in the TG content (Fig. 8G).

We then established patient derived xenograft with different SLP2 expression level to evaluate the effect of inhibiting the SLP2/ SREBP1 pathway on the growth of HCC. After verified the SLP2 expression level by WB and IHC, SLP2high PDX and SLP2low PDX were established (Fig. 8H). SLP2high PDX and SLP2low PDX mice
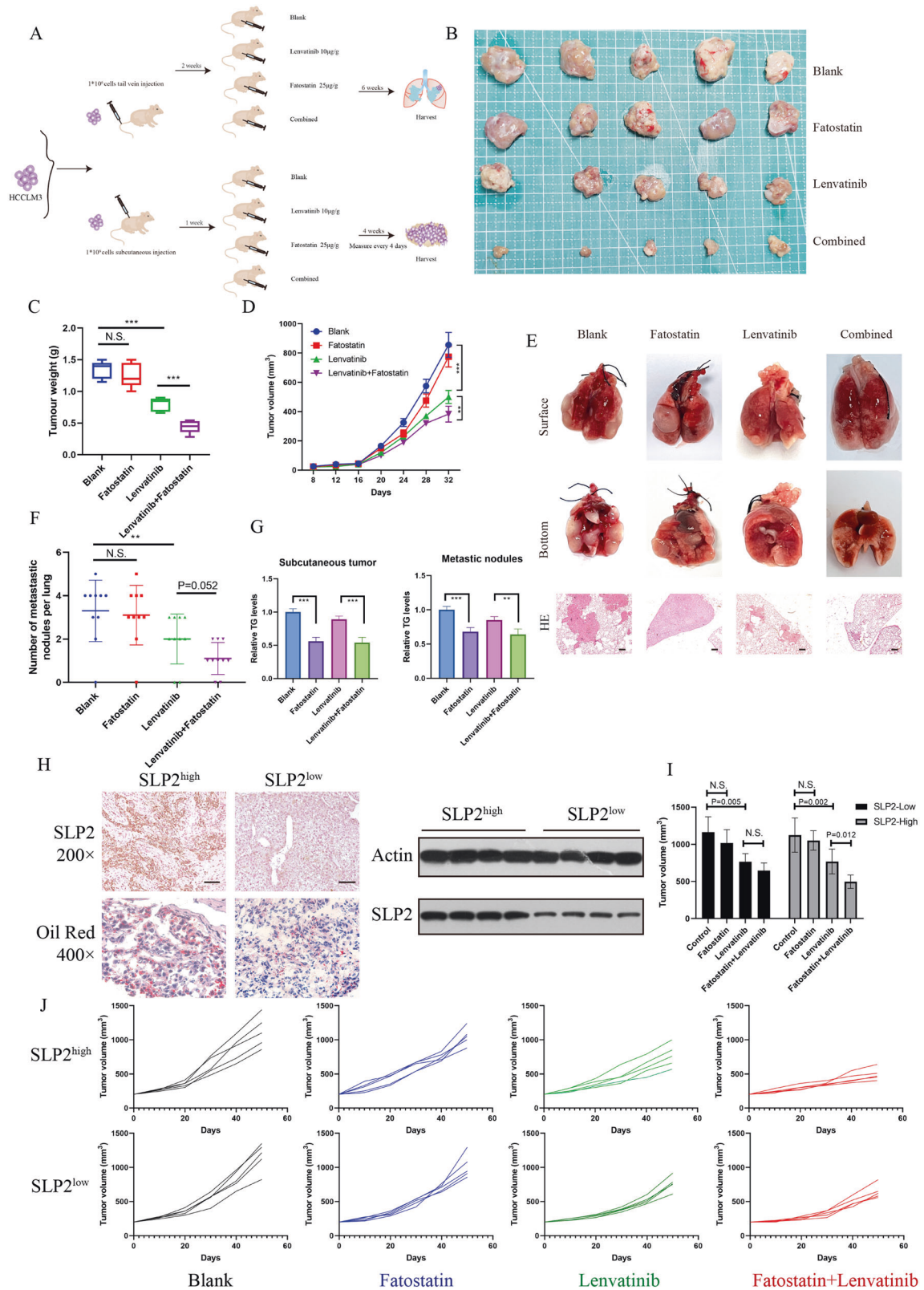
Fig. 8 **Targeting the SLP2/SREBP1 pathway effectively inhibits proliferation and metastasis of HCC tumors with high SLP2 expression in vivo. A** Treatment of nude mice in animal experiments. **B** Representative images of subcutaneous HCC tumors from each group ($n = 5$ mice/group). **C** The tumor weight of each group. **D** The dynamic change in tumor volume. **E, F** Representative images of lung metastasis specimens and H&E staining in lung metastasis specimens. scale bar: 50 μm. **G** TG levels of subcutaneous HCC tumors and metastatic nodules. **H** Representative images of SLP2 IHC staining and oil red staining in HCC tissues (left panel), scale bar: 25 μm. representative images following Western blotting of SLP2 in HCC tissues (right panel). **I, J** In PDX model, the inhibitory effects of Fatostatin and Lenvatinib on the growth of HCC were detected. *$p < 0.05$; **$p < 0.01$; ***$p < 0.001$, ****$p < 0.0001$.

were divided into four groups and received different treatment as mentioned in the previous paragraph when the tumor volume reached to approximately 200 mm^3. After 50 days treatment, the final tumor volume in the SLP2^{high} PDX group was decreased in Lenvatinib group and Lenvatinib+Fatostatin group, tumor volume in the fatostatin group was similar to that of the blank group. Importantly, minimal tumor median volume was found in the combination therapy group, indicating a significant difference compared with either drug alone or the blank group. However, in SLP2^{low} PDX group, Lenvatinib remains therapeutically effective, while combined therapy didn't result in statistically significant difference compared with the Lenvatinib group. These data indicated that inhibiting the SLP2/SREBP1 pathway in HCC cells with high SLP2 expression can effectively inhibit tumor growth, and the combined use of Fatostatin and Lenvatinib has a higher treatment efficacy.

In summary, the above in vitro and in vivo experiments, functional gain-and-loss studies, and animal model inhibitor intervention experiments suggest that SLP2 is involved in lipid metabolism, which promotes cancer cell proliferation and metastasis. Since SLP2 exerts its biological effects by regulating JNK2, the application of JNK2 inhibitors can attenuate the pro-cancer effects of SLP2. In animal experiments, Fatostatin combined with Lenvatinib inhibited tumor growth and metastasis and prolonged median OS. Overall, we conclude that SLP2 regulates the progression of HCC by promoting JNK2/SREBP1-mediated lipogenesis

DISCUSSION

HCC is considered one of the most common and deadly tumors worldwide, with high morbidity and mortality rates. Accordingly, identifying the causes of the high malignancy of HCC and corresponding therapeutic targets is the key to advancing HCC treatment. In this study, we demonstrate that SLP2 is an oncogene associated with the ability to promote proliferation and metastasis in HCC that promotes de novo lipogenesis mainly through the regulation of JNK2 and SREBP1. SLP2 can bind JNK2 to maintain JNK2 protein stability and enable it to bind SREBP1. The binding of JNK2 and SREBP1 promotes the nuclear translocation of SREBP1, which enhances the transcription of key enzymes for lipid synthesis and promotes de novo lipogenesis in HCC cells. However, this pro-cancer process could be abrogated by JNK2/SREBP1 inhibitors, and the application of SREBP1 inhibitors attenuated the proliferation and metastasis of HCC cells with high SLP2 expression. Overall, for the first time, we have revealed that SLP2 is a key factor that promotes HCC metastasis and proliferation by regulating lipid metabolism and report the inhibitory effect of JNK2/SREBP1 inhibitors on HCC cells with high SLP2 expression.

SLP2, located on the mitochondrial inner membrane, is a member of the stomatin protein family, which was recently shown to be involved in the development of tumors [25]. According to recent research, SLP2 has been implicated in the development of many malignant tumors and poor prognosis [26]. In this study, we screened SLP2 through the TCGA database as well as analysis of single-cell data and validated this finding with clinical specimens that we collected. We found that high expression of SLP2 leads to shorter survival in HCC patients.

An interesting question is how SLP2 promotes the progression of HCC. We confirmed that SLP2 can bind JNK2 via GST pull-down assays. JNK2, also known as MAPK9, belongs to the mitogen-activated protein kinase (MAPK) family. JNK2 is associated with a variety of cellular responses, including proliferation, cell stress, and cell death [27, 28]. The JNK family contains three proteins, JNK1 and JNK2, which are expressed in most human tissues, while JNK3 is found in only the brain, heart, and testis [29]. JNK1 and JNK2 have been demonstrated to be associated with the stress

response in tumor cells, regulating cell proliferation, apoptosis, and differentiation [30–32]. Since JNK1 and JNK2 are structurally similar, we clarified by co-IP experiments that SLP2 binds JNK2 but not JNK1. Moreover, the stability of JNK2 in the cytoplasm is a key factor in regulating SREBP1-mediated lipid metabolism. We first demonstrated that upregulation of SLP2 expression increased JNK2 stability and thus promoted JNK2 accumulation. Increased JNK2 could enhance SREBP1-mediated de novo lipogenesis. In contrast, SLP2 knockdown significantly reduced the stability of JNK2. These results indicate that SLP2 is a novel and important regulator of the JNK2-SREBP1 system that regulates the stability of JNK2 through direct interaction with JNK2.

In the previous studies, SLP2 has been shown to be associated with EMT as well as NF-κb pathway in hepatocellular carcinoma [18]. In another study, silencing SLP2 could suppress inflammatory response in HCC [33]. Moreover, SLP2 confers a poor prognosis for HCC and that SLP2 expression affects the migration, invasive, and proliferative potential of HCC [34]. However, the exact molecular mechanism remains unclear. We discovered lipid metabolism reprogramming as a novel mechanism of SLP2 regulation of hepatocellular carcinoma which is independent from other mechanisms. Inhibition of lipogenesis in SLP2 overexpressing hepatocellular carcinoma cell lines inhibits the proliferation and metastatic capacity, which could support that the lipid metabolism regulated by SLP2 has the greatest impact on the regulation of tumor progression rather than other pathways.

Non-alcoholic fatty liver disease (NAFLD) is the most common cause of chronic liver disease worldwide, with a higher prevalence in developed countries. Moreover, NAFLD may progress to non-alcoholic steatohepatitis (NASH), which may then lead to hepatocellular carcinoma and a range of liver function disorders. Recent study has found that JNK-P38 pathway is involved in NASH and TRIM16 could suppresses the JNK-p38 signaling pathway in NASH [35]. In the present study, we revealed the upstream proteins SLP2 that can regulate JNK and thus promote de novo lipogenesis. Therefore, high expression of SLP2 may be associated with the formation of NASH and may serve as a therapeutic target for NASH and NASH-induced hepatocellular carcinoma in the future.

It is well known that the reprogramming of lipid metabolism is characteristic of cancer cells. The reprogramming of lipid metabolism in tumor cells includes changes in fatty acid uptake, de novo lipogenesis, lipid droplet generation, and beta oxidation [36]. We confirmed that high expression levels of SLP2 are associated with tumor cell metabolic reprogramming, particularly de novo lipogenesis. In the human body, most types of tissues perform biological functions through the uptake of exogenous fatty acids, except for the liver, adipose tissue, and specific physiological processes [37]. De novo lipogenesis provides a constant supply of energy, which is vital for the diverse biological processes of tumor cells [38]. We found that HCC cells with high SLP2 expression levels showed a greater capacity for de novo lipogenesis acid synthesis and ATP production. It is well known that fatty acids are vital for cancer cells because they maintain cell membrane integrity during proliferation and can serve as a major source of energy for tumor cells during stress [39]. However, more complex mechanisms of the carcinogenic effects of fatty acids are awaiting discovery. Fatty acids inside the tumor cell can maintain membrane structure and fluidity. Certainly, increased de novo lipogenesis in tumor cells promotes saturated PL synthesis, which can increase cell membrane stiffness and protect cells from ROS-induced peroxidation [40]. Lipids can also act as pro-tumorigenic signaling molecules. For example, phosphatidic acid can interact with and stabilize mTOR, resulting in enhanced activity of mTORC1 and mTORC2 [41]. In addition to acting as signaling molecules, some lipids can regulate the microenvironment of tumor cells, as widely demonstrated in the suppression of antitumor immune responses [42]. In summary, intracellular lipids may contribute to tumor malignancy through energy production, regulation of

membrane fluidity, and acting as signaling molecules. How lipid metabolism promotes tumor metastasis remains a complex issue. SREBP1 is shown to drive a transcriptional program indicative of epithelial to mesenchymal transition (EMT) in breast cancer [43]. This could also explain why knockdown of SLP2 causes phenotype changes in EMT. It has been shown that tumor cells with high metastatic capacity are more prone to use fatty acids for energy generation [44]. Taken together, SLP2-associated lipogenesis may promote tumor metastasis by means of EMT and energy generation.

In summary, SLP2 expression is elevated in HCC tissues compared to peri-tumor tissues of the liver and is associated with poor patient prognosis. Furthermore, our study revealed the underlying biological function of SLP2 in the proliferation and metastasis of HCC. Notably, our results show for the first time that SLP2 can bind JNK2 and maintain the protein stability of JNK2, further regulating the nuclear translocation of SREBP1. SLP2 promotes the expression of key enzymes for lipid synthesis through the above pathways, thereby contributing to the proliferation and metastasis of HCC. SLP2 could become a biomarker and therapeutic target for HCC, and JNK2/SREBP1 inhibitors can be considered part of the HCC treatment regimen.

MATERIALS AND METHODS
HCC specimens
Two cohorts containing 136 patients were involved in this study (Cohort 1, $n = 100$; Cohort 2, $n = 36$). Paired HCC tissues and peri-tumor tissues were obtained during surgical operation at the First Affiliated Hospital of university of science and technology of China. Handwritten informed consent was obtained from the patients, and the research was approved by the Ethics Committee of university of science and technology of China, approval number is 2021-ky130(approval date: March 31, 2021). Tumor tissue micro-array was bought from Shanghai OUTDO biotech company. Patients were followed up after discharge to monitor survival and recurrence rates. For fresh tumor tissue, Paired HCC tissues and peri-tumor tissues were obtained between February 2019 and August 2020. And for tumor tissue micro-array. Patients were followed up from August 2013 to December 2020. OS is the time interval from the end of the operation to the patient's death or last observation.

Tumor xenografts in nude mice and NSG mice
All animal experiments were approved by the Animal Ethics Committee of university of science and technology of China. approval number is 202204031831000045626 (approval date: April 3, 2022). Nude mice were housed in an SPF room with 5 mice per cage. To prepare subcutaneous xenografts, 1×10^6 parental or treated cells ($n = 5$/group) were randomly transplanted subcutaneously into the dorsal regions of 4- to 6-week-old nude mice. Tumor size was measured every 4 days until day 28. The formula used to calculate the tumor volume was $a \times b^2 \times 0.52$, where a and b represent the tumor length and width, respectively. For in vivo lung metastasis, 1×10^6 parental or treated cells were injected into the tail vein of the mice. After 6 weeks, the mice were sacrificed, and the metastatic nodes were measured. The above samples were formalin-fixed and sectioned for subsequent experiments. For patient-derived xenografts, after obtaining fresh tumor tissue from HCC patients in the operating room, it was cut into small pieces of roughly 1 cubic millimeter under aseptic conditions. The tumors were transplanted subcutaneously into the right upper limb regions of 4- to 6-week-old NSG mice. the mice were given intraperitoneal injection of Lenvatinib (10 mg/kg qd) and Fatostatin (25 mg/kg, qd).

2.3 Hydrodynamic tail vein injection
pT3-EF1a-MYC-IRES-luciferase (MYC-luc), px330-sg-p53 (sgP53), and CMV-Sleeping Beauty 13 (SB13) were purchased from Addgene, and pT3-EF1a-SLP2-IRES was designed by the authors and constructed by General Biologicals Corporation. For hydrodynamic tail vein injection, sterilized 0.9% NaCl saline was used to mix the plasmid. For the control group, 11.4 μg of Myc-luc, 10 μg of sgP53, and 5.35 μg of SB13 were added per 2 ml of saline solution. For the SLP2 group, 11.4 μg of Myc-luc, 10 μg of SLP2, 10 μg of sgP53, and 5.35 μg of SB13 were added per 2 ml of saline solution. We used 6-week-old male C57BL/6 mice for the experiments.

Each mouse was injected with 10% of its weight in volume via the tail vein over 5–7 s. The plasmids were prepared with an Endo Free Maxi Kit (Qiagen). Two months after hydrodynamic tail vein injection, the mice were sacrificed. Tumor number and size were assessed.

Information on the primary antibodies used in western blotting is provided in Supplementary Table 1. Primer sequence information for the PCR section and the specific sequences of each shRNA are shown in Supplementary Table 2.

DATA AVAILABILITY
All data generated or analyzed during this study are included in this published article and its supplementary information files. The relevant mRNA databases can be found at the following sites. https://doi.org/10.6084/m9.figshare.20087705.

REFERENCES
1. Siegel RL, Miller KD, Fuchs HE, Jemal A. Cancer statistics, 2021. CA Cancer J Clinicians. 2021;71:7–33.
2. Rich NE, Yopp AC, Singal AG. Medical management of hepatocellular carcinoma. J Oncol Pract. 2017;13:356–64.
3. Chen Q, Shu C, Laurence AD, Chen Y, Peng BG, Zhen ZJ, et al. Effect of Huaier granule on recurrence after curative resection of HCC: a multicentre, randomised clinical trial. Gut. 2018;67:2006–16.
4. Ruf B, Heinrich B, Greten TF. Immunobiology and immunotherapy of HCC: spotlight on innate and innate-like immune cells. Cell Mol Immunol. 2021;18:112–27.
5. Faubert B, Solmonson A, DeBerardinis RJ. Metabolic reprogramming and cancer progression. Sci (N. Y, NY). 2020;368:eaaw5473.
6. Wang M, Han J, Xing H, Zhang H, Li Z, Liang L, et al. Dysregulated fatty acid metabolism in hepatocellular carcinoma. Hepatic Oncol. 2016;3:241–51.
7. Li J, Huang Q, Long X, Zhang J, Huang X, Aa J, et al. CD147 reprograms fatty acid metabolism in hepatocellular carcinoma cells through Akt/mTOR/SREBP1c and P38/PPARα pathways. J Hepatol. 2015;63:1378–89.
8. Alannan M, Fayyad-Kazan H, Trézéguet V, Merched A. Targeting lipid metabolism in liver cancer. Biochemistry. 2020;59:3951–64.
9. Nguyen P, Leray V, Diez M, Serisier S, Le Bloc'h J, Siliart B, et al. Liver lipid metabolism. J Anim Physiol Anim Nutr. 2008;92:272–83.
10. Hall Z, Chiarugi D, Charidemou E, Leslie J, Scott E, Pellegrinet L, et al. Lipid remodeling in hepatocyte proliferation and hepatocellular carcinoma. Hepatol (Baltim, Md). 2021;73:1028–44.
11. Wang MD, Wu H, Fu GB, Zhang HL, Zhou X, Tang L, et al. Acetyl-coenzyme A carboxylase alpha promotion of glucose-mediated fatty acid synthesis enhances survival of hepatocellular carcinoma in mice and patients. Hepatol (Baltim, Md). 2016;63:1272–86.
12. Mitsopoulos P, Chang YH, Wai T, König T, Dunn SD, Langer T, et al. Stomatin-like protein 2 is required for in vivo mitochondrial respiratory chain supercomplex formation and optimal cell function. Mol Cell Biol. 2015;35:1838–47.
13. Christie DA, Mitsopoulos P, Blagih J, Dunn SD, St-Pierre J, Jones RG, et al. Stomatin-like protein 2 deficiency in T cells is associated with altered mitochondrial respiration and defective CD4+ T cell responses. J Immunol (Baltim, Md: 1950). 2012;189:4349–60.
14. Wang Y, Morrow JS. Identification and characterization of human SLP-2, a novel homologue of stomatin (band 7.2b) present in erythrocytes and other tissues. J Biol Chem. 2000;275:8062–71.
15. Lapatsina L, Brand J, Poole K, Daumke O, Lewin GR. Stomatin-domain proteins. Eur J cell Biol. 2012;91:240–5.
16. Chang D, Ma K, Gong M, Cui Y, Liu ZH, Zhou XG, et al. SLP-2 overexpression is associated with tumour distant metastasis and poor prognosis in pulmonary squamous cell carcinoma. Biomarkers Biochemical Indic Exposure, Response, Susceptibility Chem. 2010;15:104–10.
17. Feng Q, Hu ZY, Liu XQ, Zhang X, Lan X, Geng YQ, et al. Stomatin-like protein 2 is involved in endometrial stromal cell proliferation and differentiation during decidualization in mice and humans. Reprod Biomed Online. 2017;34:191–202.
18. Zhu W, Li W, Geng Q, Wang X, Sun W, Jiang H, et al. Silence of stomatin-like protein 2 represses migration and invasion ability of human liver cancer cells via inhibiting the nuclear factor kappa B (NF-κB) pathway. Med Sci Monit Int Med J Exp Clin Res. 2018;24:7625–32.
19. Luo A, Kong J, Hu G, Liew CC, Xiong M, Wang X, et al. Discovery of Ca2+-relevant and differentiation-associated genes downregulated in esophageal squamous cell carcinoma using cDNA microarray. Oncogene. 2004;23:1291–9.
20. Ma W, Chen Y, Xiong W, Li W, Xu Z, Wang Y, et al. STOML2 interacts with PHB through activating MAPK signaling pathway to promote colorectal Cancer proliferation. J Exp Clin Cancer Res CR. 2021;40:359.

21. Ma W, Xu Z, Wang Y, Li W, Wei Z, Chen T, et al. A positive feedback loop of SLP2 activates MAPK signaling pathway to promote gastric cancer progression. Theranostics. 2018;8:5744–57.

22. Zheng Y, Huang C, Lu L, Yu K, Zhao J, Chen M, et al. STOML2 potentiates metastasis of hepatocellular carcinoma by promoting PINK1-mediated mitophagy and regulates sensitivity to lenvatinib. J Hematol Oncol. 2021;14:16.

23. Song L, Liu L, Wu Z, Lin C, Dai T, Yu C, et al. Knockdown of stomatin-like protein 2 (STOML2) reduces the invasive ability of glioma cells through inhibition of the NF-κB/MMP-9 pathway. J Pathol. 2012;226:534–43.

24. Ito M, Nagasawa M, Omae N, Tsunoda M, Ishiyama J, Ide T, et al. A novel JNK2/SREBP-1c pathway involved in insulin-induced fatty acid synthesis in human adipocytes. J lipid Res. 2013;54:1531–40.

25. Chao D, Ariake K, Sato S, Ohtsuka H, Takadate T, Ishida M, et al. Stomatin-like protein 2 induces metastasis by regulating the expression of a rate-limiting enzyme of the hexosamine biosynthetic pathway in pancreatic cancer. Oncol Rep. 2021;45:90.

26. Wang Y, Cao W, Yu Z, Liu Z. Downregulation of a mitochondria associated protein SLP-2 inhibits tumor cell motility, proliferation and enhances cell sensitivity to chemotherapeutic reagents. Cancer Biol Ther. 2009;8:1651–8.

27. Hammouda MB, Ford AE, Liu Y, Zhang JY. The JNK signaling pathway in inflammatory skin disorders and cancer. Cells. 2020;9:857.

28. Kumar A, Singh UK, Kini SG, Garg V, Agrawal S, Tomar PK, et al. JNK pathway signaling: a novel and smarter therapeutic targets for various biological diseases. Future Med Chem. 2015;7:2065–86.

29. Hao Q, Liu Z, Lu L, Zhang L, Zuo L. Both JNK1 and JNK2 are indispensable for sensitized extracellular matrix mineralization in IKKβ-deficient osteoblasts. Front Endocrinol. 2020;11:13.

30. Takahashi H, Ogata H, Nishigaki R, Broide DH, Karin M. Tobacco smoke promotes lung tumorigenesis by triggering IKKbeta- and JNK1-dependent inflammation. Cancer Cell. 2010;17:89–97.

31. Chen YT, Lin CW, Su CW, Yang WE, Chuang CY, Su SC, et al. Magnolol triggers caspase-mediated apoptotic cell death in human oral cancer cells through JNK1/2 and p38 pathways. Biomedicines. 2021;9:1295.

32. Lepore A, Choy PM, Lee NCW, Carella MA, Favicchio R, Briones-Orta MA, et al. Phosphorylation and stabilization of PIN1 by JNK promote intrahepatic cholangiocarcinoma growth. Hepatol (Baltim, Md). 2021;74:2561–79.

33. Pu X, Dong C, Zhu W, Li W, Jiang H. Silencing stomatin-like protein 2 attenuates tumor progression and inflammatory response through repressing CD14 in liver cancer. OncoTargets Ther. 2019;12:7361–73.

34. Jones JE, Esler WP, Patel R, Lanba A, Vera NB, Pfefferkorn JA, et al. Clinical Significance of SLP-2 in Hepatocellular Carcinoma Tissues and Its Regulation in Cancer Cell Proliferation, Migration, and EMT [Retraction]. OncoTargets Ther. 2022;15:869–70.

35. Wang L, Zhang X, Lin ZB, Yang PJ, Xu H, Duan JL, et al. Tripartite motif 16 ameliorates nonalcoholic steatohepatitis by promoting the degradation of phospho-TAK1. Cell Metab. 2021;33:1372–88.e7.

36. Pavlova NN, Thompson CB. The emerging hallmarks of cancer metabolism. Cell Metab. 2016;23:27–47.

37. Jones JE, Esler WP, Patel R, Lanba A, Vera NB, Pfefferkorn JA, et al. Inhibition of Acetyl-CoA Carboxylase 1 (ACC1) and 2 (ACC2) reduces proliferation and de novo lipogenesis of EGFRvIII human glioblastoma cells. PloS one. 2017;12:e0169566.

38. Simeone P, Tacconi S, Longo S, Lanuti P, Bravaccini S, Pirini F, et al. Expanding roles of de novo lipogenesis in breast cancer. Int J Environ Res Public Health. 2021;18:3575.

39. Koundouros N, Poulogiannis G. Reprogramming of fatty acid metabolism in cancer. Br J Cancer. 2020;122:4–22.

40. Rysman E, Brusselmans K, Scheys K, Timmermans L, Derua R, Munck S, et al. De novo lipogenesis protects cancer cells from free radicals and chemotherapeutics by promoting membrane lipid saturation. Cancer Res. 2010;70:8117–26.

41. Toschi A, Lee E, Xu L, Garcia A, Gadir N, Foster DA. Regulation of mTORC1 and mTORC2 complex assembly by phosphatidic acid: competition with rapamycin. Mol Cell Biol. 2009;29:1411–20.

42. Basingab FS, Ahmadi M, Morgan DJ. IFNγ-Dependent Interactions between ICAM-1 and LFA-1 Counteract Prostaglandin E2-Mediated Inhibition of Antitumor CTL Responses. Cancer Immunol Res. 2016;4:400–11.

43. Zhang N, Zhang H, Liu Y, Su P, Zhang J, Wang X, et al. SREBP1, targeted by miR-18a-5p, modulates epithelial-mesenchymal transition in breast cancer via forming a co-repressor complex with Snail and HDAC1/2. Cell Death Differ. 2019;26:843–59.

44. Pascual G, Avgustinova A, Mejetta S, Martín M, Castellanos A, Attolini CS, et al. Targeting metastasis-initiating cells through the fatty acid receptor CD36. Nature. 2017;541:41–5.

ACKNOWLEDGEMENTS

AUTHOR CONTRIBUTIONS

YL: formal analysis, investigation, methodology, writing – original draft. LS: investigation, data curation. HG: methodology, validation. SZ: investigation. WC: methodology, visualization. CJ: formal analysis, software. FM: methodology, validation. SL: methodology. BZ: data curation. YY: data curation. KM: validation, XL: validation, TC: validation; XG: formal analysis; NZ: formal analysis; JW: supervision; YL: writing– review & editing, methodology; LL: funding acquisition, conceptualization.

FUNDING

COMPETING INTERESTS

The authors declare no competing interests.

ADDITIONAL INFORMATION

Supplementary information The online version contains supplementary material available at https://doi.org/10.1038/s41388-022-02551-z.

Correspondence and requests for materials should be addressed to Jiabei Wang, Yao Liu or Lianxin Liu.

Reprints and permission information is available at http://www.nature.com/reprints

Publisher's note Springer Nature remains neutral with regard to jurisdictional claims in published maps and institutional affiliations.